Available online at www.sciencedirect.com
SCIENCE DIRECT®
Journal of Solid State Chemistry 178 (2005) 3414–3419
JOURNAL OF SOLID STATE CHEMISTRY
www.elsevier.com/locate/jssc

Directing the structures of silver-antimony sulphides: A new topological variant of the $[Ag_5Sb_3S_8]^{2-}$ double layer

Anthony V. Powell[a,*], Jürgen Thun[a], Ann M. Chippindale[b]

[a]*Department of Chemistry, Heriot-Watt University, Edinburgh EH14 4AS, UK*
[b]*School of Chemistry, The University of Reading, Whiteknights Reading RG6 6AD, UK*

Received 5 July 2005; received in revised form 23 August 2005; accepted 27 August 2005
Available online 30 September 2005

Abstract

A new silver–antimony sulphide, $[C_6H_{20}N_4][Ag_5Sb_3S_8]$, has been synthesised solvothermally in the presence of triethylenetetramine and characterised by single-crystal X-ray diffraction, thermogravimetry and elemental analysis. The compound crystallises in the space group $P2_1/m$ ($a = 6.2778(7)$, $b = 15.8175(16)$ and $c = 12.4617(15)$ Å and $\beta = 104.561(5)^\circ$) and adopts a structure in which honeycomb-like sheets of fused six-membered silver–antimony-sulphide rings are linked through Ag–S bonds to form double layers. The idealised structure can be considered to be derived from that of antifluorite and represents a second structure type for the $[Ag_5Sb_3S_8]^{2-}$ double layer.

Keywords: Silver–antimony sulphide; Solvothermal sythesis

1. Introduction

Interest in the application of structure-directed synthesis for the preparation of novel chalcogenides continues to grow. Adapting the methodology commonly used for the preparation of zeolites and other framework oxides, Bedard et al. [1] demonstrated that the crystallisation of tin and germanium sulphides can be effected solvothermally in the presence of an organic amine as a structure-directing agent. Subsequently, similar solvothermal reactions have successfully been carried out for sulphides of the main-group elements arsenic, antimony, indium, tin and germanium. This has led to the identification of a number of novel secondary building units such as adamantane-like $Ge_4S_{10}^{4-}$ cages [2], $In_{10}S_{20}^{10-}$ supertetrahedra [3] and $Sb_3S_6^{3-}$ semicubes [4], which have no counterparts in oxide chemistry. The structural features of these sulphides have recently been reviewed [5,6].

Whilst the precise mode of operation of the structure-directing species is not well understood, it is believed that hydrogen bonding between protonated nitrogen atoms of the amine and the typically anionic metal-sulphide framework, plays a key rôle in stabilising a given structure [7,8]. The marked tendency towards low dimensionality in antimony sulphides has stimulated efforts to incorporate transition-metal ions into the structures in an effort to generate low-dimensional magnets. However, the introduction of transition-metal ions into solvothermal reactions involving antimony sulphide generally favours the formation of salt-like materials [9], in which a cationic transition-metal complex serves to balance the charge of the anionic antimony-sulphide framework. There have been comparatively few reports of the incorporation of transition-metal ions into the main-group-sulphide matrix itself [10–12], although the later transition-series elements appear to be more readily incorporated into the primary antimony-sulphide bonding network than their early series congeners [13–17].

Reports of the synthesis in supercritical ammonia of a range of silver–antimony sulphides [16,17] suggested that structure-directed synthesis might be used to effect the crystallisation of materials in which silver is incorporated into the primary metal-sulphide bonding network.

*Corresponding author. Fax: +44 131 451 3180.
E-mail address: a.v.powell@hw.ac.uk (A.V. Powell).

0022-4596/$ - see front matter © 2005 Elsevier Inc. All rights reserved.
doi:10.1016/j.jssc.2005.08.022

Adapting this strategy, we recently succeeded in preparing, by reaction in ethylenediamine, novel silver–antimony sulphides [18]. In addition to $[C_2H_9N_2][Ag_2SbS_3]$, the structure of which is closely related to the copper–antimony chalcogenides, $[C_2H_8N_2]_x[Cu_2SbQ_3]$ ($x = 1/2$, Q = S, Se; $x = 1$, Q = Se) [14,19], a new structure type was observed in $[C_2H_9N_2]_2[Ag_5Sb_3S_8]$ [18], in the idealised form of which, cations simultaneously occupy half of the tetrahedral and all of the octahedral sites between pairs of close-packed sulphide layers.

Here we report a new variant of this layered structure, prepared in the presence of triethylenetetramine (TETN), $H_2N(CH_2)_2NH(CH_2)_2NH(CH_2)_2NH_2$. Despite the similarity between this amine and ethylenediamine, solvothermal synthesis leads to a new type of $[Ag_5Sb_3S_8]^{2-}$ double layer, in which all cations reside in tetrahedral sites. This demonstrates the complex nature of the structure-directing process, in which subtle variations in the organic species can produce marked structural changes in the metal-sulphide framework.

2. Experimental

A reaction mixture consisting of Sb_2S_3 (0.68 g, 2 mmol), $AgNO_3$ (0.17 g, 1 mmol) and S (0.16 g, 5 mmol) was loaded into a 23 ml Teflon-lined stainless-steel autoclave and 5 ml of TETN added to give a suspension with an approximate molar composition Sb_2S_3:$AgNO_3$:S:TETN of 2:1:5:34. After stirring for 10 min, the vessel was sealed and heated to 140 °C for 5 days before cooling to room temperature at a rate of 1 °C min^{-1}. Reaction mixtures with this molar composition did not produce single crystals at the higher reaction temperatures of 165 or 190 °C (at which synthesis was successfully carried out in ethylenediamine) [18], nor did reactions with Sb_2S_3:$AgNO_3$ ratios in the range 0.25–1.0. The polycrystalline products of such reactions consisted primarily of the condensed phase Ag_3SbS_3 (pyrargyrite) [20]. The product formed at 140 °C was filtered, washed successively with ethylenediamine, methanol, deionised water and acetone before drying in air at room temperature. The solid product consisted of a mixture of orange plate-like crystals of the title compound, together with a small amount of black powder. Powder X-ray diffraction data for a ground sample of the bulk material were collected with nickel-filtered Cu-K_α radiation ($\lambda = 1.5418$ Å) using a Philips PA2000 powder diffractometer. The majority of peaks in the diffraction pattern can be indexed on the basis of the monoclinic unit cell determined from the single-crystal diffraction study of the title compound, $[C_6N_4H_{20}][Ag_5Sb_3S_8]$. Peaks corresponding to Ag_3SbS_3 [20], present as the black powder, were also identified in the pattern.

The orange crystals were separated by hand-picking from the bulk product. Combustion analysis gave C 5.46%, H 1.55%, N:3.87% (calculated for $[C_6H_{20}N_4][Ag_5Sb_3S_8]$: C 5.50%, H 1.54%, N 4.28%). Thermogravimetric analysis was performed using a DuPont Instruments 951 Thermal Analyser. Approximately 9 mg of finely ground crystals were heated under a flow of dry nitrogen over the temperature range 25–290 °C at a heating rate of 2 °C min^{-1}. The single weight loss of 10.64%, whose onset is at ca. 154 °C, compares favourably with the value of 11.32% calculated for the complete removal of TETN molecules. The powder X-ray diffraction pattern of the thermal decomposition product indicates it to be predominantly Ag_3SbS_3, together with an unidentified minor phase.

2.1. Crystal structure determination

X-ray intensity data for $[C_6H_{20}N_4][Ag_5Sb_3S_8]$ were collected at room temperature using a Bruker-AXS X8 Apex2 CCD diffractometer with graphite monochromated Mo-K_α radiation ($\lambda = 0.71073$ Å). Data were processed using the manufacturer's standard routines [21]. Full crystallographic details are given in Table 1.

The structure was solved using the direct methods program SHELXS [22] and all framework atoms located. The CRYSTALS suite of programs [23] was used for subsequent refinements against F. The carbon and nitrogen atoms of the amine were located in difference Fourier maps and found to be disordered over two crystallographically inequivalent positions in the ratio 0.62(2):0.38(2). In the final cycles of refinement, anisotropic thermal parameters were refined for all framework atoms, together with isotropic parameters and site occupancies for the carbon and nitrogen atoms. Hydrogen atoms of the amine were placed geometrically after each cycle of refinement. A three-term Chebyshev polynomial was applied as the weighting scheme.

Table 1
Crystallographic data for $[C_6N_4H_{20}][Ag_5Sb_3S_8]$

Formula	$[C_6N_4H_{20}][Ag_5Sb_3S_8]$
M_r	1309.45
Crystal habit	Orange plate
Dimensions/mm	$0.3 \times 0.3 \times 0.05$
Crystal system	Monoclinic
Space group	$P2_1/m$
T/K	293
a/Å	6.2778(7)
b/Å	15.8175(16)
c/Å	12.4617(15)
β/°	104.561(5)
V/Å^3	1197.7(2)
Z	2
Wavelength/Å	0.71073
μ/cm^{-1}	8.026
ρ/g cm^{-3}	3.631
Measured data	37031
Unique data	3780
Observed data ($I > 3\sigma(I)$)	3125
R_{merg}/%	3.00
R/%	2.86
R_w/%	3.40

Crystallographic data (excluding structure factors) have been deposited with the Cambridge Crystallographic Data Centre as supplementary publication no. CCDC 277056. Copies of the data can be obtained, free of charge, on application to CCDC, 12 Union Road, Cambridge CB2 1EZ, UK (fax: +44 1223 336033 or email:deposit@ccdc.cam.ac.uk).

3. Results and discussion

The atomic coordinates and isotropic thermal parameters of the non-hydrogen atoms of $[C_6H_{20}N_4][Ag_5Sb_3S_8]$ are presented in Table 2 and the local coordination of the framework atoms is shown in Fig. 1. Selected bond lengths and angles appear in Table 3. The compound crystallises in a new structure type, consisting of silver–antimony-sulphide double layers separated by organic cations, that is related to that of $[C_2H_9N_2]_2[Ag_5Sb_3S_8]$ [18]. Both of the crystallographically distinct antimony atoms are coordinated to three sulphur atoms at distances in the range 2.394(1)–2.5008(9) Å in an approximately trigonal pyramidal geometry with S–Sb–S angles of between 89.85(5)–101.16(5)°. Trigonal pyramidal SbS_3^{3-} primary building units of this type are commonly observed in the structures of antimony sulphides prepared under solvothermal conditions but $[C_6H_{20}N_4][Ag_5Sb_3S_8]$ is somewhat unusual in not exhibiting any significant secondary Sb…S interactions at distances within the sum of the van der Waals' radii of Sb and S (3.80 Å) [24]. Of the three crystallographically distinct silver atoms, both Ag(1) and Ag(2) exhibit a distorted tetrahedral coordination, with mean Ag–S distances of ca. 2.64 Å, comparable to values in the literature for silver sulphides with tetrahedral coordination [25]. Ag(3) however, has only three sulphur atoms within bonding distance, 2.483(1)–2.573(1) Å, and has approximately trigonal planar coordination by sulphur, with S–Ag–S angles lying in the range 99.99(4)–131.89(5)°. In addition to its presence in $[C_2H_9N_2]_2[Ag_5Sb_3S_8]$, described previously [18], trigonal planar coordination of silver has been reported in materials such as $CsAg_7S_4$ [26] and KAg_5S_3 [27]. Bond-valence sums [28] (Table 3) are consistent with formal valence states of Ag(I) and Sb(III) resulting in doubly negatively charged silver–antimony-sulphide layers.

Vertex linking of the SbS_3, AgS_4 and AgS_3 units produces six-membered rings, in which metal and sulphur

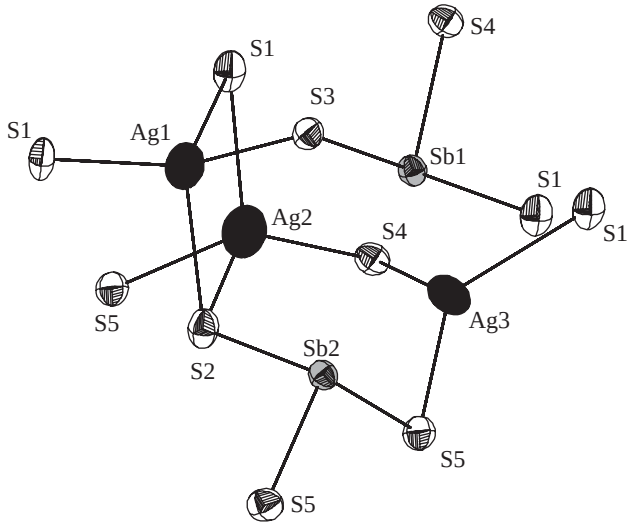

Fig. 1. Local coordination of the framework atoms showing the atom labelling scheme and ellipsoids at 50% probability.

Table 2
Fractional atomic coordinates and equivalent isotropic thermal parameters (Å^2) for non-hydrogen atoms in $[C_6N_4H_{20}][Ag_5Sb_3S_8]$

Atom	x	y	z	U_{iso}	Occ[a]
Ag(1)	0.7192(1)	0.75	0.53088(7)	0.0461	
Ag(2)	0.7126(1)	0.60182(3)	0.35144(6)	0.0534	
Ag(3)	0.20056(9)	0.52157(3)	0.32871(5)	0.0469	
Sb(1)	0.28678(5)	0.61412(2)	0.55742(3)	0.0218	
Sb(2)	0.12403(7)	0.75	0.32986(4)	0.0215	
S(1)	0.9075(2)	0.60676(8)	0.5696(1)	0.0315	
S(2)	0.5043(3)	0.75	0.3164(2)	0.0301	
S(3)	0.4086(3)	0.75	0.6565(2)	0.0255	
S(4)	0.4605(2)	0.53727(8)	0.7216(1)	0.0277	
S(5)	−0.0234(2)	0.63259(8)	0.2114(1)	0.0297	
C(10)	0.829(2)	0.406(1)	0.056(1)	0.067(4)	0.62(2)
C(11)	0.907(4)	0.415(1)	0.086(2)	0.063(6)	0.38(2)
C(20)	0.591(3)	0.407(1)	−0.016(1)	0.074(5)	0.62(2)
C(21)	0.705(3)	0.406(1)	−0.013(2)	0.051(5)	0.38(2)
C(30)	1.110(3)	0.2986(2)	0.120(2)	0.105(7)	0.62(2)
C(31)	1.063(3)	0.2987(2)	0.169(2)	0.061(6)	0.38(2)
N(10)	0.913(2)	0.3406(8)	0.143(1)	0.055(3)	0.62(2)
N(11)	0.837(3)	0.3348(9)	0.130(1)	0.033(3)	0.38(2)
N(20)	0.534(3)	0.325(1)	−0.077(1)	0.094(6)	0.62(2)
N(21)	0.512(3)	0.361(1)	0.011(2)	0.062(6)	0.38(2)

[a]The site occupancy factors are 1.00 unless stated otherwise.

Table 3
Selected bond lengths (Å), angles (°) and bond valences (v.u.) for $[C_6N_4H_{20}][Ag_5Sb_3S_8]$

		v*			v*			v*
Ag(1)–S(1)	2.545(1)	0.34	Ag(2)–S(1)	2.687(2)	0.23	Ag(3)–S(1)^{b}	2.573(1)	0.31
Ag(1)–S(1)^{a}	2.545(1)	0.34	Ag(2)–S(2)	2.666(1)	0.24	Ag(3)–S(4)^{b}	2.542(1)	0.34
Ag(1)–S(2)	2.674(2)	0.24	Ag(2)–S(4)^{b}	2.521(1)	0.36	Ag(3)–S(5)	2.483(1)	0.40
Ag(1)–S(3)	2.791(2)	0.17	Ag(2)–S(5)^{c}	2.736(2)	0.20			
		1.09			1.03			1.05
Sb(1)–S(1)^{d}	2.426(1)	1.06	Sb(2)–S(2)	2.435(2)	1.04			
Sb(1)–S(3)	2.5008(9)	0.87	Sb(2)–S(5)	2.408(1)	1.12			
Sb(1)–S(4)	2.394(1)	1.16	Sb(2)–S(5)^{a}	2.408(1)	1.12			
		3.09			3.28			
S(1)–Ag(1)–S(1)^{a}	125.82(7)		S(1)–Ag(2)–S(2)	102.71(6)		S(1)^{b}–Ag(3)–S(4)^{b}	99.99(4)	
S(1)–Ag(1)–S(2)	106.44(4)		S(1)–Ag(2)–S(4)^{b}	115.86(5)		S(1)^{b}–Ag(3)–S(5)	131.89(5)	
S(1)^{a}–Ag(1)–S(2)	106.44(4)		S(1)–Ag(2)–S(5)^{b}	116.46(4)		S(4)^{b}–Ag(3)–S(5)	119.93(5)	
S(1)^{a}–Ag(1)–S(3)	104.50(4)		S(2)–Ag(2)–S(4)^{b}	123.98(5)				
S(2)–Ag(1)–S(3)	108.21(6)		S(2)–Ag(2)–S(5)^{c}	95.17(5)				
			S(4)^{b}–Ag(2)–S(5)^{c}	101.54(5)				
S(1)^{d}–Sb(1)–S(3)	101.16(5)		S(2)–Sb(2)–S(5)	100.96(5)				
S(1)^{d}–Sb(1)–S(4)	99.53(5)		S(2)–Sb(2)–S(5)^{a}	100.96(5)				
S(3)–Sb(1)–S(4)	89.85(5)		S(5)–Sb(1)–S(5)^{a}	100.94(7)				

Note: Symmetry transformations used to generate equivalent atoms: ^{a}x, $3/2-y$, z, $^{b}1-x$, $1-y$, $1-z$, $^{c}1+x$, y, z, and $^{d}x-1$, y, z.
*Bond valences and their sums calculated using parameters from Ref. [28].

atoms alternate. Two types of ring may be identified: the majority, seven eighths, contain two Ag atoms and one Sb, but one-eighth of the rings contain one Ag atom and two Sb atoms. This gives rise to the $[Ag_5Sb_3S_8]^{2-}$ stoichiometry of the honeycomb-like sheets, each of which is generated through fusion of the six-membered metal-sulphur rings. Pairs of sheets are linked through the remaining vertex of each of the $Ag(1)S_4$ and $Ag(2)S_4$ tetrahedra to form buckled double layers (Fig. 2) of stoichiometry $[Ag_5Sb_3S_8]^{2-}$, which lie parallel to the *ab* crystallographic plane. Within the double layers, the positions of the sulphur atoms correspond to an approximately AB arrangement of a close packed array of anions. Protonated TETN cations are located in the space between the double layers (Fig. 3), which are stacked along [0 0 1] with successive double layers separated by ca. 6.3 Å. Although hydrogen atoms cannot be located directly, charge balancing requires that the organic cations are diprotonated. Each atom of the protonated amine is disordered over two crystallographic sites. Disorder of the organic cation has previously been observed in Sb–S materials [9,18,29]. The long-chain diprotonated TETN adopts a conformation such that each molecule assumes the shape of the letter 'C', with both of the primary nitrogen atoms being directed at one neighbouring layer and the secondary nitrogen atoms at the other. Nearest-neighbour protonated amines in the [1 0 0] direction are all of the same orientation, whilst in the [0 1 0] direction, the orientation of organic cations alternates, with the centre of neighbouring molecular cations being displaced by [1/2 0 0] with respect to each other. All nitrogen atoms of the organic cation have sulphur neighbours at sufficiently short distances (3.17–3.57 Å) to suggest that hydrogen bonding

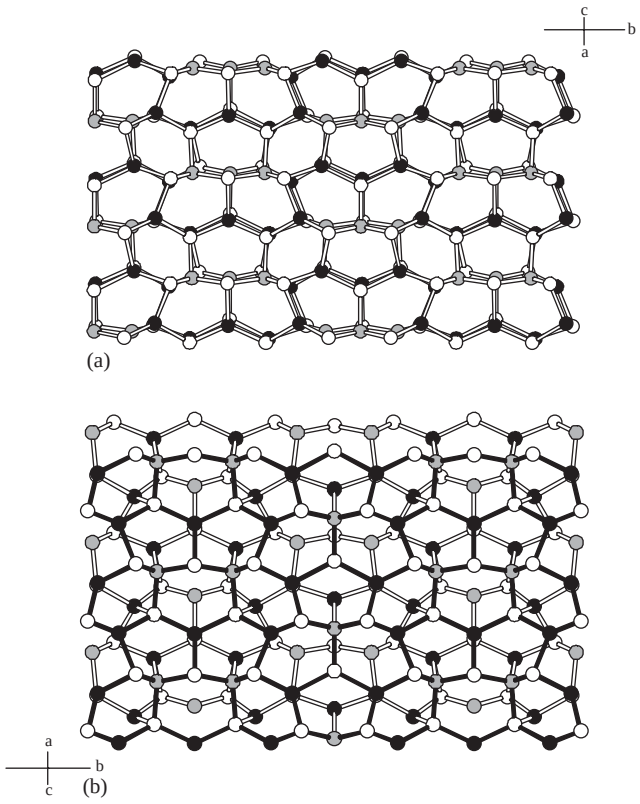

Fig. 2. View along the [1 0 1] direction of (a) an $[Ag_5Sb_3S_8]^{2-}$ double layer in $[C_6H_{20}N_4][Ag_5Sb_3S_8]$ formed from linkage through Ag–S bonds of a pair of crystallographically equivalent honeycomb-like sheets of fused six-membered silver–antimony sulphide rings and (b) the analogous $[Ag_5Sb_3S_8]^{2-}$ double layer in $[C_2H_9N_2]_2[Ag_5Sb_3S_8]$ [16], with bonds in the upper sheet shown as solid lines and those in the lower sheet as open lines. Key: silver, black circles; antimony, shaded circles; sulphur, open circles.

occurs between the diprotonated TETN and the anionic framework.

Whilst the honeycomb-like sheets present in $[C_6H_{20}N_4][Ag_5Sb_3S_8]$ are analogous to those identified in the structure of $[C_2H_9N_2]_2[Ag_5Sb_3S_8]$ [18], very different double layers are generated in the two cases. The structures of both compounds may be considered to be derived from the antifluorite structure, through excision of a block two anion layers thick parallel to the (1 1 1) crystallographic plane, which corresponds to a pair of AB close packed anion layers with all interstitial sites occupied by cations.

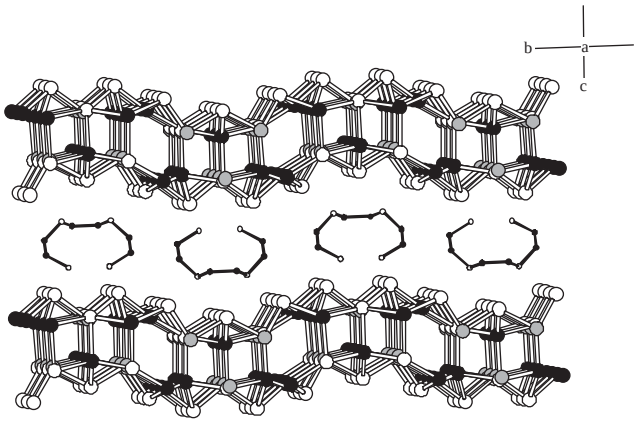

Fig. 3. View along the [1 0 0] direction of a pair of buckled $[Ag_5Sb_3S_8]^{2-}$ double layers with the diprotonated triethylenetetramine cations located in the interlayer space. Only the higher occupancy conformer of the amine is shown. Key: silver, large black circles; antimony, large shaded circles; sulphur, large open circles; carbon, small black circles; nitrogen, small open circles.

The structure of $[C_6H_{20}N_4][Ag_5Sb_3S_8]$ is a distortion of this idealised arrangement, involving deformation of the anionic layers. In particular, the buckling of the layers lowers the coordination number at those sites occupied by Sb and Ag(3), resulting respectively in effective trigonal pyramidal and trigonal planar coordination by sulphur. The structure of $[C_6H_{20}N_4][Ag_5Sb_3S_8]$ therefore shows similarities to that of $[Mn(en)_3][Ag_6Sn_2Te_8]$ [30], and may be considered as a disordered variant of the latter in which silver and tin are ordered over tetrahedral sites (Fig. 4).

By contrast, as we have previously reported [18], the idealised structure of $[C_2H_9N_2]_2[Ag_5Sb_3S_8]$ may be thought of as an ordered-defect variant of the Li_3Bi structure in which, between a pair of close-packed layers, only half of the available tetrahedral sites are occupied by cations, the remaining cations being located in octahedral positions. A buckling of the double layers similar to that observed here for $[C_6H_{20}N_4][Ag_5Sb_3S_8]$ leads to an effective trigonal planar coordination of Ag and Sb at the latter positions.

A further difference between the two compounds lies in the connectivity of the honeycomb sheets to form double layers. In $[C_2H_9N_2]_2[Ag_5Sb_3S_8]$, this is effected by metal-sulphur bonds and through short (<3.0 Å) Ag–Sb bonds, whereas in $[C_6H_{20}N_4][Ag_5Sb_3S_8]$ reported here, the shortest intermetallic contact of 3.1279(6) Å, for Ag(3)…Sb(1), is considerably longer than the shortest separation of ca. 2.9 Å in the alloy Ag_3Sb [31], indicating that there are no significant intermetallic interactions present and therefore linkage of the honeycomb sheets is exclusively through Ag–S linkages. Perhaps the most immediately noticeable difference between the structures of $[C_2H_9N_2]_2[Ag_5Sb_3S_8]$ and $[C_6H_{20}N_4][Ag_5Sb_3S_8]$ that results from the different

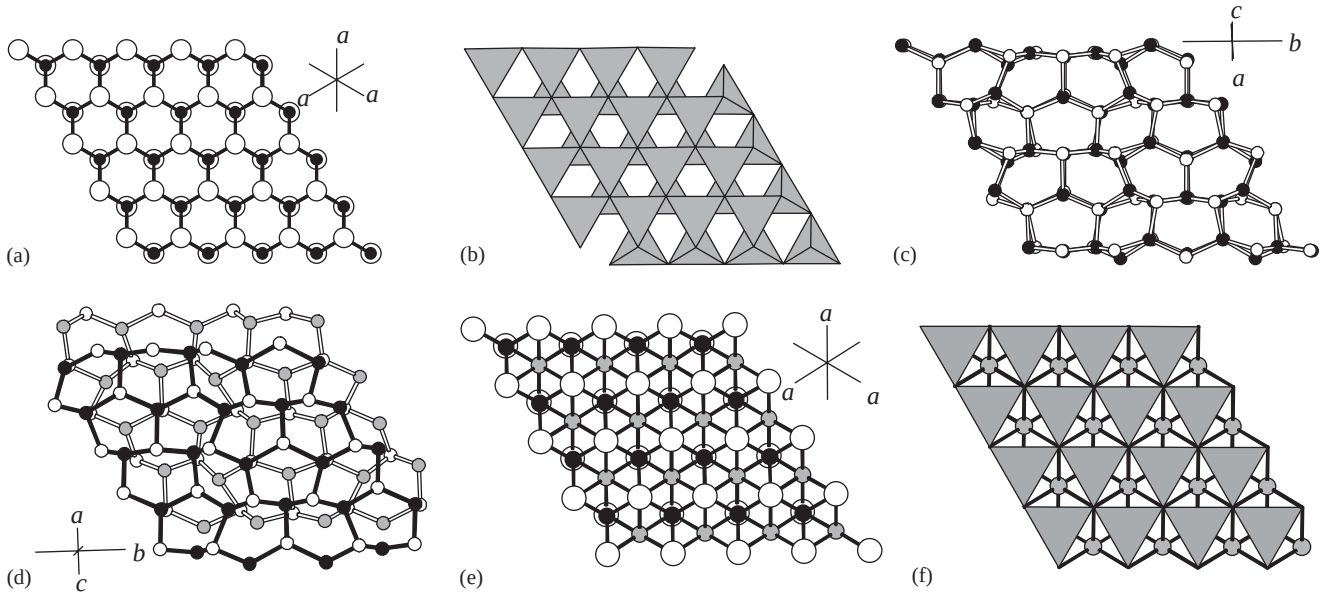

Fig. 4. The topological relationship between a block of the antifluorite structure two anion layers thick cut parallel to the (1 1 1) crystallographic plane, shown in (a) ball and stick and (b) polyhedral representations, (c) the double of layer of $[Ag_5Sb_3S_8]^{2-}$ in $[C_6H_{20}N_4][Ag_5Sb_3S_8]$ and (d) that in $[C_2H_9N_2]_2[Ag_5Sb_3S_8]$ [18], with the idealised structure of the latter shown in (e) ball and stick and (f) polyhedral representations. Key: tetrahedral sites, black circles; sulphur, open circles, octahedral sites, shaded circles.

cation coordination geometries is the apparently more open network of the double layers in $[C_6H_{20}N_4][Ag_5Sb_3S_8]$ compared to those of $[C_6H_{20}N_4][Ag_5Sb_3S_8]$ (Fig. 2). However, as atom–atom distances across the six-membered rings of the honeycomb sheets are of the order of ca. 3.9 Å, there is no significant porosity in the sheets when allowance is made for the radii of the component atoms.

In conclusion, we report here a new silver–antimony sulphide, whose idealised structure is related to a block of antifluorite. The present material, prepared in TETN, contains an $[Ag_5Sb_3S_8]^{2-}$ anion that is a topological variant of one previously prepared in ethylenediamine. The two anions differ in the coordination of the cations in the idealised structures. Preparation of these two structural variants illustrates the complexity of structure-directed synthesis: a change in reactant stoichiometry together with the relatively subtle structural variations introduced by replacement of ethylenediamine by TETN, is sufficient to enable crystallisation of a material containing a new structural variant of the $[Ag_5Sb_3S_8]^{2-}$ anion, to be effected at a markedly lower temperature than that required for synthesis in ethylenediamine. Whilst the precise mode of operation of the structure-directing agent remains unclear, the slightly lower pH of the S/TETN reaction mixture compared to that of S/en suggests that the degree of solubilzation of the inorganic components under the basic conditions of the reaction may play a rôle.

Acknowledgments

AMC thanks The Leverhulme Trust for a Research Fellowship and AVP thanks the UK EPSRC for a grant in support of a single-crystal CCD diffractometer.

References

[1] R.L. Bedard, S.T. Wilson, L.D. Vail, J.M. Bennett, E.M. Flanigen, in: P. Jacobs, R.A. van Santen (Eds.), Zeolites: Facts, Figures, Future, Elsevier, Amsterdam, 1989.
[2] M. MacLachlan, N. Coombs, G.A. Ozin, Nature 397 (1999) 681.
[3] C.L. Cahill, K. Younghee, J.B. Parise, Chem. Mater. 10 (1998) 19.
[4] K. Tan, Y. Ko, J.B. Parise, J.B. Park, A. Darovsky, Chem. Mater. 8 (1996) 2510.
[5] W.S. Sheldrick, J. Chem. Soc., Dalton Trans. (2000) 3041.
[6] J. Li, Z. Chen, R.J. Wang, D.M. Proserpio, Coord. Chem. Rev. 190–192 (1999) 707.
[7] L. Engelke, C. Näther, W. Bensch, Eur. J. Inorg. Chem. (2002) 2936.
[8] R. Kiebach, F. Studt, C. Näther, W. Bensch, Eur. J. Inorg. Chem. (2004) 2553.
[9] H.-O. Stephan, M.G. Kanatzidis, Inorg. Chem. 36 (1997) 6050.
[10] H.-O. Stephan, M.G. Kanatzidis, J. Am. Chem. Soc. 118 (1996) 12226.
[11] L. Engelke, M. Schaefer, M. Schur, W. Bensch, Chem. Mater. 13 (2001) 1383.
[12] R. Kiebach, W. Bensch, R.-D. Hoffmann, R. Pöttgen, Z. Anorg. Allg. Chem. 629 (2003) 532.
[13] G.L. Schimek, J.W. Kolis, G.J. Long, Chem. Mater. 9 (1997) 2776.
[14] A.V. Powell, S. Boissière, A.M. Chippindale, J. Chem. Soc., Dalton Trans. (2000) 4192.
[15] A.V. Powell, R. Paniagua, P. Vaqueiro, A.M. Chippindale, Chem. Mater. 14 (2002) 1220.
[16] G.L. Schimek, W.T. Pennington, P.T. Wood, J.W. Kolis, J. Solid State Chem. 123 (1996) 277.
[17] P.T. Wood, G.L. Schimek, J.W. Kolis, Chem. Mater. 8 (1996) 721.
[18] P. Vaqueiro, A.M. Chippindale, A.R. Cowley, A.V. Powell, Inorg. Chem. 42 (2003) 7846.
[19] Z. Chen, R.E. Dilks, R. Wang, J.Y. Lu, J. Li, Chem. Mater. 10 (1998) 3184.
[20] D.J. Harker, Chem. Phys. 4 (1936) 381.
[21] Apex-2 Software, Bruker-AXS, 2004, Madison, Wisconsin, USA.
[22] G.M. Sheldrick, in: SHELXS97. Program for the Solution of Crystal Structures, University of Gottingen, Federal Republic of Germany, 1997.
[23] D.J. Watkin, C.K. Prout, J.R. Carruthers, P.W. Betteridge, R.I. Cooper, in: CRYSTALS Issue 11, Chemical Crystallography Laboratory, University of Oxford, UK, 2001.
[24] A. Bondi, J. Phys. Chem. 69 (1964) 441.
[25] M. Auernhammer, H. Effenberger, E. Irran, F. Pertlik, J. Rosenstingl, J. Solid State Chem. 106 (1993) 421.
[26] P.T. Wood, W.T. Pennington, J.W. Kolis, Inorg. Chem. 33 (1994) 1556.
[27] M. Emirdag, G.L. Schimek, J.W. Kolis, Acta Crystallogr. C 54 (1998) 1376.
[28] N.E. Brese, M. O'Keefe, Acta Crystallogr. B 47 (1991) 192.
[29] A. Puls, M. Schaefer, C. Näther, W. Bensch, A.V. Powell, S. Boissière, A.M. Chippindale, J. Solid State Chem. 178 (2005) 1171.
[30] A. Chen, R.J. Wang, J. Li, Chem. Mater. 12 (2000) 762.
[31] J.D. Scott, Can. Mineral. 14 (1976) 139.